

ANATOLII A. GALUSHKO¹
HELENA SOVOVÁ²
ROUMIANA P. STATEVA¹

¹Institute of Chemical
Engineering, Bulgarian Academy
of Sciences, Sofia, Bulgaria

²Institute of Chemical Process
Fundamentals, Prague,
Czech Republic

SCIENTIFIC PAPER

633.822+546.26431:541.8+66.011

SOLUBILITY OF MENTHOL IN PRESSURISED CARBON DIOXIDE – EXPERIMENTAL DATA AND THERMODYNAMIC MODELLING

The paper reports new experimental data and the results of the thermodynamic modelling of menthol solubility in pressurised CO₂. The solubility was measured using the dynamic method and modelled with the Soave–Redlich–Kwong equation of state in the temperature range 30–60 °C and pressure range 66–144 bar. The results obtained were compared with the solubility data published by Maier and Stephan and by Sovová and Jež. The agreement with Maier and Stephan was very good: The deviation of the solubilities, published by Sovová and Jež, from the other data sources was explained and revised accordingly. The paper also presents for the first time experimental and modelling data for the melting point depression of menthol in the presence of carbon dioxide in the pressure range of interest up to 60 bars. The experimental data was obtained comparing the appearance of menthol particles before and after their exposure to pressurised carbon dioxide.

Key words: Menthol, Carbon dioxide, Solubility, Melting point depression, Thermodynamic modelling.

Menthol, C₁₀H₁₈O, is a saturated secondary alcohol. Naturally occurring (–)-menthol (or *l*-menthol), an optical isomer of specific rotation –48°, is together with menthone the major component in peppermint oil, the popular flavour used in a wide range of sugar confectioneries, chewing gums, toothpastes, chocolate fillings, pharmaceuticals and liqueurs. One appealing possibility for obtaining peppermint oil from vegetable material is extraction with supercritical carbon dioxide, which is a green solvent and its solvent power and selectivity can be manipulated by small variations in pressure and temperature in order to optimally utilize its potential. Goto et al. [1] studied the supercritical fluid extraction of essential oil from peppermint leaves and measured the solubility of pure *l*-menthol in supercritical CO₂. They found the solubility of menthol extracted from the leaves to be much lower than the solubility of pure menthol, probably as a result of its interaction with the vegetable matrix. Still, the knowledge of pure menthol solubility in supercritical CO₂ is essential for understanding the process and several other papers have been devoted to its experimental measurement [2–4]. However, the agreement of the data from different sources is rather poor.

This study reports new information on the solubility of menthol in pressurised CO₂, gives results of its thermodynamic modelling and validates them against our experimental data and the data obtained by other authors. The paper also presents for the first time experimental data on the melting point depression for the menthol + CO₂ system and the thermodynamic

modelling of the solid + liquid + gas equilibria in the pressure and temperature intervals of interest to the experiment.

EXPERIMENTAL

Chemicals

Optically active (–)-menthol was supplied by Sigma-Aldrich Chemie GmbH. Menthol, a mixture of isomers (purity >98%) was obtained from Fluka Chemie AG. Carbon dioxide for food industry (purity > 97 vol.%) was purchased from Linde Technoplyn.

Solubility measurement

The solubility of menthol in dense CO₂ was measured using a flow-type apparatus (Figure 1).

CO₂ from a pressure bottle was further pressurised to operating pressure using a syringe pump or a compressor with a pressure control unit at its outlet. It flowed to the saturator – a high-pressure column of 12 ml volume and 8 mm inner diameter filled with of 2 g menthol and glass beads 2 mm in diameter. Menthol

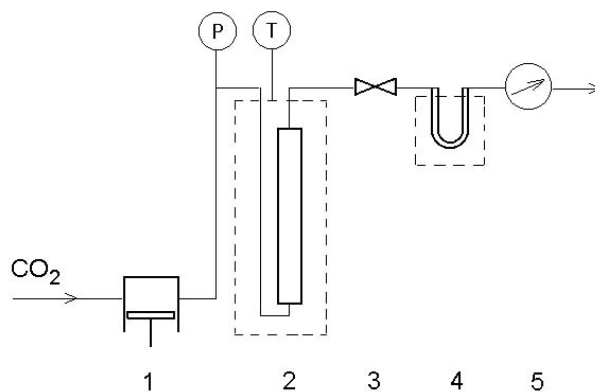


Figure 1. Scheme of a flow-type apparatus. (1) syringe pump; (2) saturator; (3) heated micrometer valve; (4) trap; (5) gas meter

Paper presented at the 1st South–East European Congress of Chemical Engineering, Belgrade, September 25–28, 2005

Author address: H. Sovová, ^bInstitute of Chemical Process Fundamentals, Rozvojová 135, 16502 Prague 6, Czech Republic

E-mail address: sovoval@icpf.cas.cz

Paper received: September 19, 2006

Paper accepted: February 5, 2006

was filled into the column at ambient conditions in the form of crystals or powder, but after equipment pressurisation with carbon dioxide it became liquid. Thin layers of glass wool were put on the bottom of the column to prevent loss of the powder and on the top to prevent menthol entrainment as liquid droplets with the vapour phase flowing out of the saturator. The saturator was submerged in a water bath with temperature controlled within $\pm 0.1^\circ\text{C}$.

The supercritical fluid saturated with menthol was depressurised through a home-made micrometer valve that was electrically heated to compensate for the heat consumption during gas expansion. The valve was designed to minimise the dead volume and thus to reduce the amount of solute that could settle in the valve as it precipitated from the solution during expansion.

Menthol and gaseous CO_2 from the valve outlet were introduced into a trap, a U-shaped glass tube with glass wool preventing entrainment from the outlet where menthol was collected. The trap was either at room temperature or was cooled in a dry ice + ethanol bath. The volume of CO_2 flowing out of the separator was measured at ambient conditions by a gas meter (Spectrum Skutec). The pressure at the saturator inlet was measured using a digital manometer (Stöfl Mess- und Sensortechnik) with an accuracy of ± 0.1 bar. The pressure changes during a run ranged from 0.2 to 0.8 bar, depending on the amount of solvent consumed during the run. The mean pressure value was used in the evaluation of the run. The CO_2 flow rate for each measurement was $0.1\text{--}0.2\text{ g} \cdot \text{min}^{-1}$. It was proved in preliminary tests that this flow rate was slow enough to ensure the complete saturation of CO_2 with menthol at the saturator outlet.

When a sufficient amount of menthol was collected in the trap, the flow rate was stopped and menthol was determined by mass using an analytical balance (accuracy ± 0.1 mg). The solubility was calculated from the amounts of the collected solute and of the gas. The temperature in the saturator was $30\text{--}60^\circ\text{C}$, the pressure was varied between 63 and 144 bar. Three to five measurements were carried out for each set of conditions.

Menthol state determination

To determine the state of menthol (either solid or liquid) the same equipment was used as for the solubility measurement. The saturator was filled with glass beads almost to half of its height, and then a layer of menthol particles was placed on filter paper and covered with another piece of filter paper. The rest of the space was filled with glass beads, the saturator was closed, immersed in a temperature bath, rinsed with low-pressure carbon dioxide and then slowly pressurised up to the pressure required. After 15 min it was slowly depressurised and the menthol particles that remained between the filter papers were taken out,

examined under a microscope, and compared with the particles that were not treated with carbon dioxide. The beads from the saturator were also examined.

EXPERIMENTAL RESULTS

Solubility

The results of the solubility measurement obtained in this study are listed in Table 1.

Table 1. Solubility of menthol in carbon dioxide (mole fraction)

P (bar)	$10^3 y$	P (bar)	$10^3 y$	P (bar)	$10^3 y$
T = 303 K					
66.4	0.35	76.1	23.4		
71.5–72.1 ^a	14.2	91.8	35.3		
T = 313 K					
75.0	0.68	86.6	8.80	92.4	16.5
75.6	0.70	88.0	10.8	93.3	20.1
78.6	0.93	88.7	11.9	94.2	18.2
80.9	1.55	89.6	12.7	96.6	24.7
83.9	4.21	89.9	13.5	100.3	24.5
85.8	6.57	90.0	13.8	102.3	27.4
86.1	8.83	90.2	14.1	107.7	34.5
86.3	8.74	90.8	14.9		
86.4	9.70	91.2	16.2		
T = 323 K					
76.5	0.56	97.3	3.79	117.1	18.0
82.7	0.65	105.7	8.10	121.3	23.4
88.3	1.04	105.8	9.21	123.3	24.5
93.3	1.83	113.7	18.1		
T = 333 K					
75.5	0.70	93.4	1.32	143.7	39.8
83.7	0.73	112.0	3.73		
86.1	0.73	125.7	14.2		

^aThe pressure and temperature could not be maintained with sufficient accuracy in the region where CO_2 evaporates.

When the solubilities of (–)-menthol and of the mixture of menthol isomers were compared, no differences were found. Also, the concentrations measured either with a cooled trap or with a trap at room temperature were equal as long as the mole fractions were higher than $1 \cdot 10^{-3}$. At lower menthol concentrations, however, the amount of menthol dissolved in gaseous carbon dioxide at room temperature, and thus escaping with the gas from the trap, was no longer negligible compared to the amount of trapped menthol. Thus, Table 1 shows only the data measured with the cooled trap in this region. The relative standard deviation of the solubility data, estimated from the reproducibility of the individual experimental runs, was better than 6% except for the mole fractions lower

than $7 \cdot 10^{-4}$. The solubility data at 30°C is published for the first time. The number of experimental points is limited because of the sharp change in the solubility near the critical point of CO₂, between 70 and 75 bar, where the pressure and temperature in the saturator fluctuated during each single measurement.

We compared the results of the dynamic solubility measurement listed in Table 1 with all the data available at the temperatures of interest on menthol solubility in dense CO₂. The best agreement was observed with the data published by Maier and Stephan [2], who used as an equilibrium cell an autoclave equipped with a special device for vapour-phase sampling, enabling direct injection into a gas chromatograph. The measurement in this set-up seems to be free of systematic error. The menthol solubilities published by Sovová and Jež [3] were systematically lower than the previously mentioned results. They were measured in an apparatus almost identical to the one described in this work using, however, a different type of manometer. Only after the paper was published was it found that the adjustable zero of the manometer was accidentally shifted and all the pressure readings were by 2.5 bar higher than the real pressure values. Hence, the pressure values given in ref. [3] were revised by subtracting 2.5 bar from each pressure value for the purpose of a clear graphical comparison with this work (see Figure 2). The data [1,4] seem to be affected by experimental error as they deviate from the other results and from each other substantially. They were, therefore, not included in the comparison.

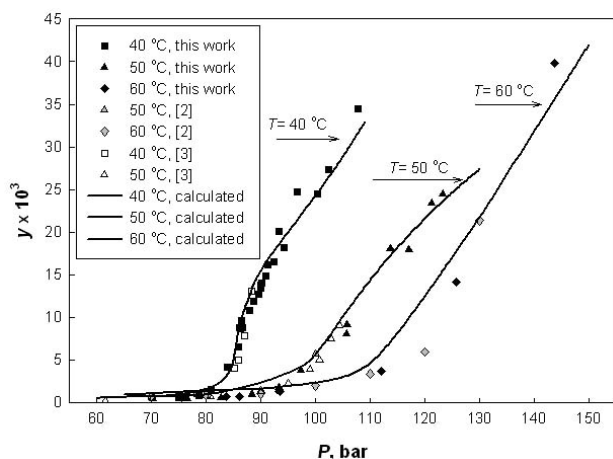


Figure 2. Menthol solubility in dense CO₂. Model calculations: (---) $k_{ij} = 0.132$ for $T = 313.2$ K, $k_{ij} = 0.1407$ for $T = 323.2$ K, and $k_{ij} = 0.151$ for $T = 333.2$ K

Menthol state

There were three cases observed when the content of the depressurised saturator was examined. In the first case, the shape and the size of the particles remained almost unchanged and menthol was found neither on the glass beads nor on the inner walls of the

saturator; hence, it was concluded that menthol was solid and dissolved very slowly in CO₂. In the second case, the menthol particles were either amorphous or they formed a layer on the paper after exposure, and some menthol was found outside the space limited by the filter papers. Thus, menthol was both melting and dissolving in CO₂. And finally in the third case, most of the menthol was found outside the space, only traces of amorphous menthol were left on the filter paper, and there was an intensive smell of menthol when the saturator was depressurised. Therefore, menthol was melting and dissolving in CO₂ and the mass transfer rate was much higher than in the second case. Thus, by changing the pressure in the range 15–61 bar and the temperature in the range 15–31°C, we were able to approximately assess the borders of the regions of similar behaviour of menthol in contact with pressurised carbon dioxide. The results will be shown together with the results of thermodynamic modelling in a subsequent section of the paper.

THERMODYNAMIC MODELLING

In the presence of a solvent, the melting curve of the solid solute can be depressed. The increase of the ideal partial molar entropy of the solute in the liquid phase, because of the dissolution of the solvent in the liquid solute, is the main reason for lowering its melting point.

There are cases known for which the depression of the melting point of the solute in the presence of a solvent is very pronounced. Lemert and Johnson [5] cite a melting point depression of up to 70 °C for 2-naphthol in the presence of methanol as a solvent. If this fact is not taken into consideration, and particularly when there is no optical view cell to observe the sample, then there is a strong possibility to mistakenly accept and report the experimental data as solid–fluid equilibrium, while in reality it is vapour–liquid and there is no solid present.

This possibility is even stronger in the cases when the melting temperature of the solute is in a close proximity of the solvent critical temperature. For example, the solubility measurement for naphthalene (melting temperature 353.65 K) at 338.1 K in supercritical CO₂ was initially reported to represent the solid–fluid equilibrium, because it was not realised that the experiment was carried out at temperatures in the vapour–liquid region. It was only later acknowledged that this measurement actually represented the composition of the vapour phase in equilibrium with a liquid and that there was no solid present [6].

For the system studied in the present work the difference between the critical temperature of the solvent CO₂ (304.2 K) and the melting temperature of the solute menthol (316.65 K, ref. [7]) was less than 13 K. Furthermore, some of the experiments were carried out at temperatures lower than the menthol melting temperature. In view of the above, it is of great

importance to know in which thermodynamic region phase the measurements were actually performed – in the vapour+solid region or in the vapour+liquid one. Ideally, to obtain an unequivocal answer to this identification problem would require reliable experimental data and information about the system's PT diagram.

However, to the best of our knowledge there are no studies on the global phase diagram of the CO₂+menthol binary, and no experimental data available about menthol melting point depression in the presence of CO₂. Thus, one should rely on model predictions, but predicting the complete PT diagram of menthol+CO₂ is a complex task and is very much outside the scope of the present study. Still, in order to alleviate the identification problem, we predicted and traced part of the CO₂+menthol SLV equilibrium line. Our predictions were then compared against the experimental data for the state of menthol, reported in the previous paragraph.

Once there is reliable information about the melting behaviour of menthol in the presence of CO₂ it is then possible to model and correctly interpret the solubility data of menthol in pressurised CO₂ at the temperatures of interest.

To successfully complete these tasks, a thermodynamic model, algorithms and numerical procedures are required, as well as information about the thermophysical properties of pure menthol.

Menthol properties

Though menthol is an abundant substance, there are limited data available in the literature on its thermophysical properties [8]. For example, in the Chemistry WebBook, NIST Standard Reference Database (<http://webbook.nist.gov/chemistry/>), the normal boiling temperature, the temperature and the heat of fusion, the critical temperature, etc. for menthol can be found. The melting temperature and the heat of fusion for menthol are also given in a handbook [7]. Values for menthol critical temperature and pressure can be found in the databases of some process simulators, for example HYSYS 3.1. (ref. [9]). All the menthol property values, used in the present study, are given in Table 2, with the references of the sources from which they were taken.

The model applied

In our study we used the Soave–Redlich–Kwong (SRK) cubic equation of state (EOS) with the one fluid van der Waals mixing rule to model the melting point depression of menthol, and its solubility in pressurised carbon dioxide:

$$P = \frac{RT}{v-b} - \frac{a}{v(v+b)} \quad (1)$$

The one fluid van der Waals mixing rule is:

$$a_{\text{mix}} = \sum_i \sum_j x_i x_j a_{ij} \quad (2)$$

$$b_{\text{mix}} = \sum_i \sum_j x_i x_j b_{ij} \quad (3)$$

where a_{mix} and b_{mix} are, the mixture energy and co-volume parameter of the EOS respectively. Usually, a geometric mean rule is applied to determine the cross-energy parameter a_{ij} :

$$a_{ij} = (a_i a_j)^{0.5} (1 - k_{ij}) \quad (2a)$$

and either an arithmetic mean (conventional linear rule):

$$b_{\text{mix}} = \sum_{i=1}^{N_c} x_i b_{ii} \quad (3a)$$

or a quadratic rule for the cross-co-volume parameter:

$$b_{ij} = \left(\frac{b_{ii} + b_{jj}}{2} \right) (1 - l_{ij}) \quad (3b)$$

Solid–liquid–vapour equilibria – modelling of the melting point depression

When three phases, namely solid, liquid and vapour are in equilibrium the following equations must be satisfied:

$$T^S = T^L = T^V \quad (4)$$

$$P^S = P^L = P^{VD} \quad (5)$$

$$f_i^S = f_i^L = f_i^V \quad i = 1, 2 \quad (6)$$

The liquid–vapour equilibrium conditions for the CO₂+menthol binary system, applying the above equations, are:

$$\phi_1^L x_1 = \phi_1^V y_1 \quad (7)$$

$$\phi_2^L x_2 = \phi_2^V y_2 \quad (8)$$

where subscript 1 corresponds to CO₂, and subscript 2 to menthol. Furthermore, it is assumed that the solid phase is pure solute, and hence for the solid–liquid equilibrium the following holds:

$$\phi_2^S = \phi_2^L x_2 \quad (9)$$

The following constraints also apply for the liquid and vapour phases:

$$\sum_{i=1}^2 x_i = 1 \quad (10)$$

$$\sum_{i=1}^2 y_i = 1 \quad (10a)$$

To calculate the fugacity coefficients of the components in the liquid and vapour phases (Eq. 7, 8) the SRK EOS with the conventional linear rule for the co-volume parameter (Eq. 3a) was applied.

The CO₂+menthol binary interaction parameter k_{ij} (Eq. 2a) was estimated to be 0.1172 minimizing the standard objective function given below:

$$F = \sum_{i=1}^{N_{\text{exp}}} |y_2^{\text{exp}} - y_2^{\text{cal}}|_i \quad (11)$$

where the number of experimental data points N_{exp} included all the data measured in this work as well as other reliable literature experimental data sources [2,3] (with a revision of the data [3] as explained above).

However, because in general EoS are not capable of representing the behaviour of the solid phase, a separate description for the fugacity coefficient of the solid was introduced [10]:

$$\ln \varphi_2^{\text{S}} = \ln \varphi_2^{\text{PSL}} + \frac{\Delta H_{\text{TP}}}{R} \left(\frac{1}{T_{\text{TP}}} - \frac{1}{T} \right) + \frac{\Delta V_{\text{TP}}}{RT} (P - P_{\text{TP}}) + \frac{\Delta C_{\text{P}}}{R} \left(\frac{T_{\text{TP}}}{T} - 1 \right) + \frac{\Delta C_{\text{P}}}{R} \ln \frac{T_{\text{TP}}}{T} \quad (12)$$

The five terms on the right-hand side of Eq. (12) are not of equal importance; the first three terms are the dominant ones and the remaining two, of opposite sign, have a tendency to approximately cancel each other out. Therefore, Eq. (12) can be simplified to the following equation:

$$\ln \varphi_2^{\text{S}} = \ln \varphi_2^{\text{PSL}} + \frac{\Delta H_{\text{TP}}}{R} \left(\frac{1}{T_{\text{TP}}} - \frac{1}{T} \right) + \frac{\Delta V_{\text{TP}}}{RT} (P - P_{\text{TP}}) \quad (13)$$

Eq. (13) relates the fugacity coefficient of the solid solute to the fugacity coefficient of the sub-cooled liquid at temperature and pressure. Hence, the data which are required for calculating the fugacity coefficient of the pure solid phase are the enthalpy of fusion at the triple point (ΔH_{TP}), the triple point temperature (T_{TP}), the triple point pressure (P_{TP}), the change in molar volume assumed to be a constant upon fusion (ΔV_{TP}), and the fugacity coefficient of the pure solute in the sub-cooled liquid phase at temperature T and pressure P (φ_2^{PSL}).

Taking into consideration that for most substances there is little difference between the triple-point temperature and the normal melting temperature, and that the difference in the heats of fusion at these two temperatures is often negligible [10], it is thus possible to estimate the reference pressure at the melting temperature of menthol (316.65 K) from an EOS.

Furthermore, a value for the solid volume of menthol is needed to estimate ΔV_{TP} . Taking into consideration that the solid density at the triple point is usually estimated for organic compounds as 1.17 times the liquid density at the triple point [7], the solid volume of menthol was estimated to be $156 \text{ cm}^3/\text{mol}$ (see Table 2).

Finally, the fugacity coefficient of the pure solute in the sub-cooled liquid phase was also calculated from the EOS.

To trace the SLV line for the binary system of CO_2 +menthol, a pressure value must be specified, and Eqs. (7), (8) and (13) must be solved for the temperature and one composition in the liquid and the vapour phases. The system of equations is strongly non-linear and may have several solutions. The non-uniqueness is a particular problem and is a result of the mathematical

Table 2. The properties of Menthol ($\text{C}_{10}\text{H}_{10}\text{O}$)

Property	Value	Source
Molecular weight	156.27	
Melting point (K)	316.65	Perry and Green [7]
ΔH fusion (J/mol)	12189.07	Perry and Green [7]
T_{C} (K)	658	HYSYS [9]
P_{C} (bar)	27.104	HYSYS [9]
V^{S} (cm^3/mol)	156	Estimated
P_{TP} (bar)	0.009535	Calculated
Acentric factor	0.7796	HYSYS[9]

presence of local minima and maxima in the Gibbs energy surface. This, in turn, relates to convergence to a local rather than global minimum, and to the impossibility to distinguish among thermodynamically stable, and unstable equilibrium states. Taking into consideration that the equality of the chemical potentials represents a necessary but not sufficient condition for equilibrium, a stability analysis routine [11], based on a modified tangent-plane function [12] and a phase identification procedure, was employed. Thus, a phase configuration with a minimum Gibbs energy was guaranteed to be found, which is particularly important in thermodynamic phase regions where the EOS has multiple roots as is the case around the SLV conditions.

Part of the CO_2 +menthol SLV equilibrium line predicted is depicted in Figure 3. The comparison of our predictions with the experimental data for the state of menthol demonstrates very good agreement.

Solubility correlation

According to our modelling results, confirmed by the menthol state analysis experiments, the solubility measurements of menthol at the temperatures and

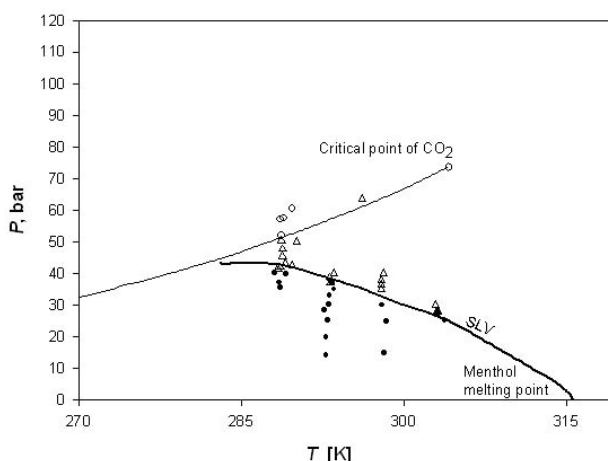


Figure 3. Menthol melting point depression in the presence of CO_2 . Experiment: (●) solid; (Δ) melted and dissolved; (\circ) melted and dissolved with higher mass transfer rate. Thermodynamic modelling: (—) vapour pressure curve of CO_2 ; (---) SLV equilibrium line

pressures of interest were performed in the vapour–liquid region, with no solid phase present. Hence, a vapour–liquid flash routine combined with a stability analysis procedure as discussed originally by Stateva and Tsvetkov[12] was applied to calculate the concentration of menthol in the vapour and liquid equilibrium phases.

In our preliminary investigations (not shown here owing to lack of space), it was found that the introduction of the size binary interaction parameter l_{ij} (Eq. (3b)) had no pronounced influence on the quality of the predictions, and thus the conventional linear rule for the co–volume parameter (Eq. 3a) was applied. Hence, for each temperature, only the value of the energy parameter k_{ij} (Eq. 2a) was determined minimizing the standard objective function (Eq. 11). The corresponding values obtained were $k_{ij} = 0.132$ for $T = 313.2$ K, $k_{ij} = 0.1407$ for $T = 323.2$ K, and $k_{ij} = 0.151$ for $T = 333.2$ K.

The comparison between the solubility of menthol in pressurised CO_2 , calculated by the SRK cubic EOS, with the experimental data obtained in this study and the data of ref. [2,3] are presented in Figure 2. The average absolute relative deviation (AARD, % = $100F/N_{\text{exp}}$) between the experimentally measured solubility data in this work and the data calculated by the thermodynamic model was less than 5% for all three temperatures.

CONCLUSION

The present paper reports new experimental data on the solubility of menthol in pressurised CO_2 . The SRK EOS was employed to model the solubility, and the results obtained were validated against the data measured in this study and against the data of other authors.

Furthermore, for the first time the melting point depression of menthol in the presence of CO_2 was predicted in the regions of interest and the results obtained were compared with the experimental assessment of the state of menthol in the same regions, and showed very good agreement.

ACKNOWLEDGEMENTS

This work was supported by the Grant Agency of the Academy of Sciences of the Czech Republic (Project No. A4072102). The authors thank M. Koptová for her experimental assistance.

NOMENCLATURE

a_{mix}	mixture energy parameter of the SRK–EOS
a_{ij}	SRK–EOS cross–energy parameter
b_{mix}	co–volume parameter of the SRK–EOS
b_{ij}	SRK–EOS cross–co–volume parameter
ΔC_p	change in the specific heat assumed to be a constant upon fusion
f_i	fugacity of the i -th component
F	objective function
ΔH_{TP}	enthalpy of fusion at the triple point

k_{ij}	SRK EOS energy binary interaction parameter
l_{ij}	SRK EOS size interaction parameter
N_{exp}	number of experimental data points for a given temperature
P	pressure
R	universal gas constant
T	temperature
v	molar volume
ΔV_{TP}	the change in volume assumed to be a constant upon fusion
x	mole fraction in the liquid phase
y	mole fraction in the vapour phase

Greek letters

ϕ	fugacity coefficient
ω	acentric factor

Subscripts

c	critical
mix	corresponding to the mixture
TP	triple point

Superscripts

cal	calculated
exp	experimental
L	liquid phase
PSL	pure sub–cooled liquid
S	solid phase
V	vapour phase

REFERENCES

- [1] M. Goto, M. Sato, T. Hirose, Extraction of peppermint oil by supercritical carbon dioxide, *J. Chem. Eng. Japan*, **26** (1993) 401–407.
- [2] M. Maier, K. Stephan, Eine neue Apparatur zur Messung der Löslichkeit von organischen Stoffen in hochverdichteten Gasen, *Chem. Ing. Tech.*, **56** (1984) 222–223.
- [3] H. Sovová, J. Jeř, Solubility of menthol in supercritical carbon dioxide, *J. Chem. Eng. Data*, **39** (1994) 840–841.
- [4] M. Mukhopadhyay, S.K. De, Fluid phase behavior of close molecular weight fine chemicals with supercritical carbon dioxide, *J. Chem. Eng. Data*, **40** (1995) 909–913.
- [5] R.M. Lemert and K.M. Johnston, Solid–Liquid–Gas Equilibria in Multicomponent Supercritical Fluid Systems, *Fluid Phase Equilibria*, **45** (1989) 265–286.
- [6] G. Xu, A.M. Scurto, M. Castier, J.F. Brennecke, M.A. Stadtherr, Reliable computation of high–pressure solid–fluid equilibrium, *Ind. Eng. Chem. Res.*, **39** (2000) 1624–1636.
- [7] R.H. Perry, D.W. Green, *Perry's Chemical Engineers' Handbook*, McGraw Hill, New York (1999), p.155.
- [8] C. Becker, H. Reiss, R.H. Heist, Estimation of thermophysical properties of a large polar molecule and application to homogeneous nucleation of l–menthol, *J. Chem. Phys.*, **68** (1978) 3585–3594.
- [9] HYSYS. Version 3.1. Copyright© 1996–2003, AspenTech.
- [10] J.M. Prausnitz, R.N. Lichtenthaler, E.G. Azevedo, *Molecular Thermodynamics of Fluid–Phase Equilibria*, Prentice Hall, Englewood Cliffs N.J. 1999, pp. 671–749.

- [11] W.A. Wakeham, R.P. Stateva, Numerical Solution of the Isothermal Multiphase Flash Problem, *Reviews in Chemical Engineering*, **20** (2004) 1–56.
- [12] R.P. Stateva, St. Tsvetkov, A Diverse Approach for the Solution of the Isothermal Multiphase Flash Problem. Application to Vapor–Liquid–Liquid Systems, *Can. J. Chem. Eng.*, **72** (1994) 772–734.

IZVOD

RASTVORLJIVOST MENTOLA U KOMPRIMOVANOM UGLJEN DIOKSIDU – EKSPERIMENTALNI PODACI I TERMODINAMIČKI MODEL

(Naučni rad)

Anatolii A. Galushko¹, Helena Sovová², Roumiana P. Stateva¹

¹Institut za hemijsko inženjerstvo, Bugarska akademija nauka, Sofija, Bugarska

²Institut za istraživanje fundamentalnih osnova hemijskih procesa, Prag, Češka Republika

U radu se navode novi eksperimentalni podaci i rezultati termodinamičkog modela kojim je definisana rastvorljivost mentola u komprimovanom CO₂. Rastvorljivost je merena primenom dinamičke metode, a model je razvijen na osnovu Soave–Redlich–Kwong jednačine stanja za uslove 30–60 °C i 66–144 bar. Dobijeni podaci su upoređeni sa do sada publikovanim u literaturi pri čemu su oni koje su objavili Maier i Stephan slažu sa rezultatima ovih ispitivanja, ali je istovremeno ukazano i u ovom radu objašnjeno na neslaganje sa podacima koje su ranije objavili Sovova i Jež. Ovaj rad, takođe, po prvi put eksperimentalno verifikuje i teorijskim modelom objašnjava sniženje temperature topljenja mentola u prisustvu ugljen dioksida na pritiscima iznad 60 bara. Eksperimentalni podaci o temperaturi topljenja mentola su određeni poređenjem stvaranja čestica mentola pre i nakon dovođenja mentola u kontakt sa komprimovanim ugljen dioksidom.

Ključne reči: Mentol, Ugljen dioksid, Rastvorljivost, Sniženje temperature topljenja, Termodinamički model.